THE STRUCTURE OF THE LOWER TRANSITION REGION AS INFERRED FROM THE HYDROGEN LYMAN-α LINE RADIANCE

L. Teriaca, U. Schühle, S.K. Solanki, W. Curdt, E. Marsch

Max-Planck-Institut für Sonnensystemforschung, Max-Planck Str. 2, 37191 Katlenburg-Lindau, Germany.
Emails: teriaca@mpsi.mpg.de

ABSTRACT

The hydrogen Lyman lines dominate the Vacuum UltraViolet (VUV) radiance spectrum of the Sun and the resonance (α) line at 121.6 nm, in particular, dominates the solar radiative losses around 20,000 K.
Using the SUMER spectrograph aboard SOHO, we have built simultaneous raster scans in H I Ly-α and in the optically thin Si III 120.6 nm line (T ≈ 60,000 K). The images look quite similar at the SUMER spatial resolution of 1.5″, showing the integrated H I Ly-α radiance to be a good diagnostic of the lower transition region. The radiance frequency distribution of the H I Ly-α line is fairly well represented by a lognormal function, although the fit is not as good as in the case of mid-transition-region lines. The average size of network structures seen in H I Ly-α is consistent with that seen in other lines formed at similar temperatures, but larger than in lines formed around 10^5 K.

1. INTRODUCTION

The Lyman-α ($1s\ ^2S_{1/2} - 2p\ ^2P_{3/2,1/2}$) transitions of neutral hydrogen are responsible for the strongest emission line in the solar spectrum and dominate the radiative losses for the temperature regime between 8,000 K and 30,000 K. Hence, H I Ly-α is the most important line formed in the lower transition region (TR) and upper chromosphere. This is the region where the expansion of the photospheric magnetic field takes place, and it is extremely important for studies of the coupling of the solar outer atmosphere with the underlying photosphere.

Although this line is optically thick, it was already shown 25 years ago by the Transition Region Camera (TRC: Bonnet et al. 1980) Lyman-α imager that structures were still not resolved at 1″ resolution. More recently, the Very high-resolution Advanced Ultraviolet Telescope (VAULT: Korendyke et al. 2001) Lyman-α spectroheliograph has revealed structures as small as its 0.33″ (≈ 240 km) resolution. Such images also show many structures evolving on time scales of few tens of seconds. Thus, H I Ly-α can provide powerful diagnostics for studying the region between the upper chromosphere and the lower transition region.
The quiet solar atmosphere is characterized by a pattern of bright and dark areas known as network and cell centers, respectively. The network originates from the advection of the photospheric magnetic flux towards the edges of the supergranulation cells by convective motions.
The photospheric magnetic network can be identified in the radiance pattern of all the lines formed at temperatures ranging from the chromosphere ($T\approx10^4$ K), up to the corona ($T\approx10^6$ K). The classical picture of the solar corona is based on the idea that the photospheric magnetic field expands rapidly with height, thus forming funnels which fill the whole corona and form a canopy of horizontal field lines above the cell centers (Gabriel 1976). The inability of such a model to reproduce the amount of emission observed from lines formed at transition region temperatures ($T\approx10^5$ K) has led to the proposal that a large number of cold ($T\leq10^5$ K) loops must also be present together with the hotter coronal funnels (e.g., Dowdy et al. 1986).

Table 1: Summary of the quiet Sun H I Ly-α observations.

Date	Solar coordinates at sequence start[(a)]	Start UTC (duration min)	Exposure time (s)	Type of Sequence	Spectral lines (λ in nm)
14 April 2005	X=200, Y=179 X=284. Y=179	13:26:22 (60) 14:28:39 (47)	10 10	E-W raster W-E raster	Ly-α λ121.567 N V λ 123.882, O V λ 62.973
15 April 2005	X=0, Y=29 X=85. Y=29	15:30:08 (12) 15:43:18 (22)	3 15	E-W raster W-E raster	Ly-α λ 121.567 N V λ 123.882, O V λ 62.973
16 April 2005	X=0, Y=29 X=85. Y=29	22:12:13 (20) 22:33:56 (22)	10 15	E-W raster W-E raster	Ly-α λ 121.567, Si III λ 120.651 N V λ 123.882, O V λ 62.973
18 April 2005	X=260, Y=29 X=345. Y=29	18:53:20 (20) 19:15:02 (22)	10 15	E-W raster W-E raster	Ly-α λ 121.567, Si III λ 120.651 N V λ 123.882, O V λ 62.973
01 June 2005	X=−43, Y=29	22:31:22 (11)	7.5	E-W raster	Ly-α λ 121.567, Si III λ 120.651
01 June 2005	X=−43, Y=29	22:58:06 (11)	7.5	E-W raster	Ly-α λ 121.567, Si III λ 120.651

(a) Coordinates refer to the centre of the useable part of the detector covered by the slit.

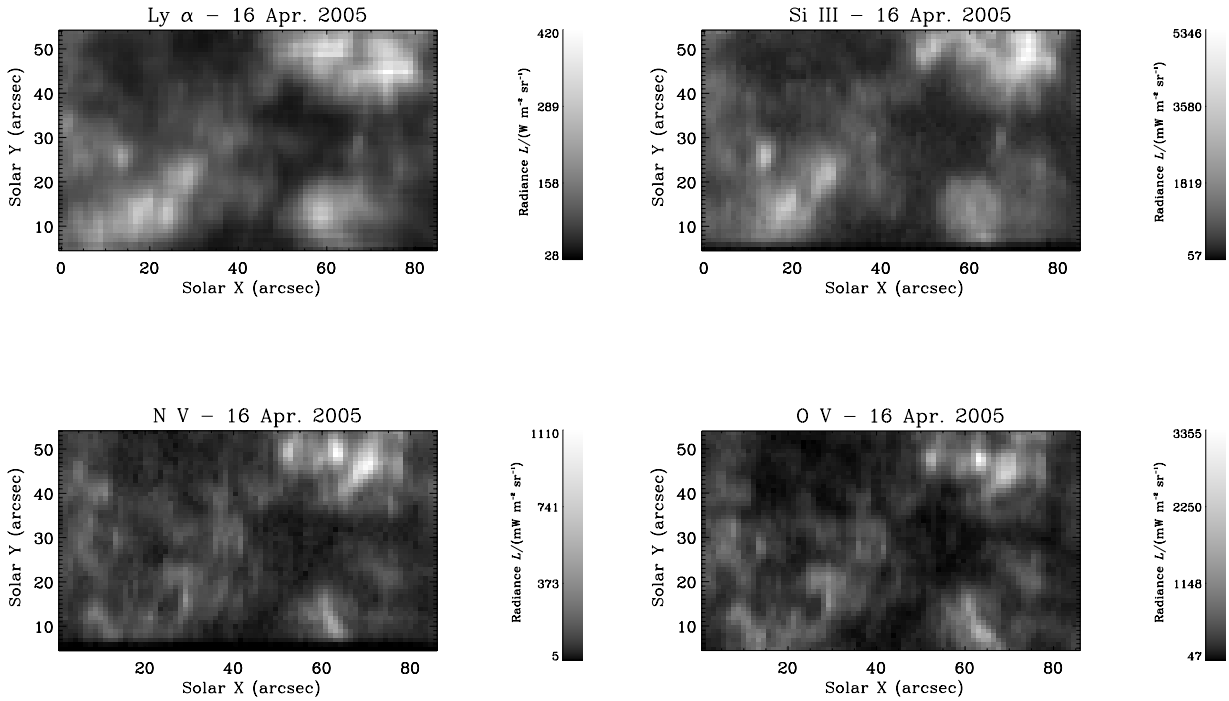

Figure 1. Square-root radiance images of a quiet region near Sun centre. The H I Ly-α and Si III images are simultaneous in time and space, and appear remarkably similar despite the large optical thickness of H I Ly-α. The images in the two hotter lines (N V and O V) show quite more structures and dynamics.

In such models the presence of the cold loops helps to confine the magnetic field, which therefore expands much less rapidly with height at chromospheric level, as compared with Gabriel's model. Such a scenario seems to be confirmed by recent force-free field extrapolations (Schrijver & Title 2003; Tu et al. 2005). The study of the network expansion with increasing temperature may help in discriminating between these different scenarios.

High spatial and spectral resolution observations in the H I Ly-α line were obtained in the past by instruments in Earth's orbit and were, hence, deeply affected by the presence of strong geocoronal absorption (Fontenla et al. 1988).

The SUMER instrument aboard SOHO (located at the first Lagrangian point) is well outside the hydrogen geocorona. This, together with the precise radiometric calibration of the instrument, permits us to study the morphology and dynamics of the lower transition region in its dominant emission line with unprecedented detail and accuracy. Furthermore, the high spectral resolution of SUMER allows us to analyze the H I Ly-α profile in different locations of the solar disk. This will be presented in a separate paper. Here we focus only on the morphology and structure seen in H I Ly-α images.

2. OBSERVATIONS

Small raster scans (≈ 80″×58″) of selected quiet Sun areas have been produced with the SUMER spectrograph (Wilhelm et al. 1995) aboard SOHO. Since May 2004 detector A has been showing a deterioration of the ADC in the time-to-digital converter box. As a consequence, large portions of the detector can only be used binned over 64 spatial pixels. This defect concerns only the y–ADC, affecting the spatial information, while the x–ADC is working correctly, leading to correct spectral information. Presently, only the 58 rows at the bottom of the detector still retain their full spatial resolution (≈1″) and were used for the present study. The defect appears progressing also when the detector is turned off. This has led to the decision of allowing, for the first time since the beginning of the mission, on-disk observations of the H I Ly-α line to be made outside of the attenuator areas. A summary of all the data used in this paper is given in Table 1.

Due to the continuously changing detector conditions, special attention needs to be paid to the data reduction process. The flat-fields, in particular, have been obtained by averaging and median filtering large amounts of data. All data were acquired using the narrow 0.3″×120″ slit on the bottom part of detector A.

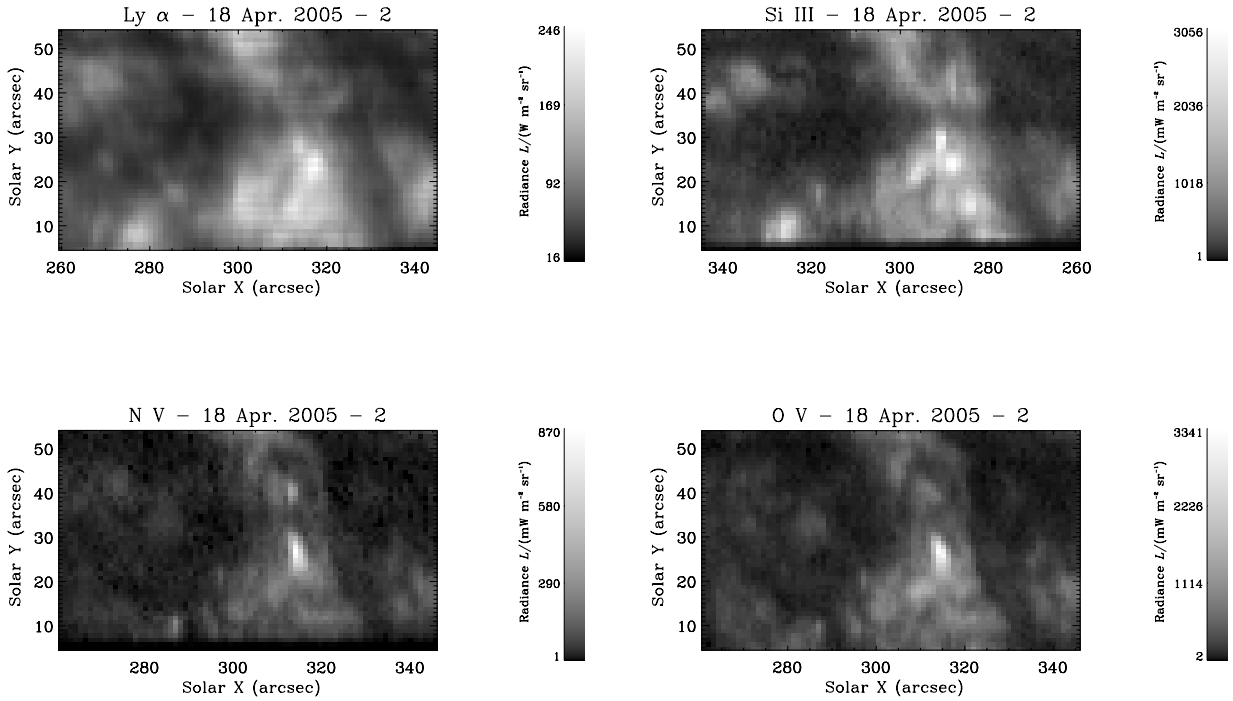

Figure 2. As in Figure 1, the H I Ly-α and Si III images appear quite similar, although the latter shows sharper features.

3. MORPHOLOGY OF THE LOWER TR

Figures 1 and 2 show the network structures of the quiet Sun in H I Ly-α as compared to images obtained in the optically thin lines Si III λ120.6 (6×10^4 K), N V λ123.8 (1.8×10^5 K), and O V λ62.97 (2.5×10^5 K). The data in Si III λ120.6, in particular, are obtained simultaneously in time and space to that in H I Ly-α and reveal a close similarity despite the large opacity of the H I Ly-α line. The images in O V and N V show more structuring and more spatial variations. It is unclear how much of this difference is due to larger temporal variations in N V and O V. Figure 3 shows a raster scan obtained by stepping the 0.3″ wide slit westward by 0.37″ after each exposure, thus achieving a slightly better spatial resolution in the direction perpendicular to the slit.

4. RADIANCE FREQUENCY DISTRIBUTION

In early studies, the observed radiance frequency distribution (hereafter RFD) of VUV lines were fitted by two Gaussians, thus attempting a separation between cell centres and network lanes (e.g., Reeves 1976). More recently, Pauluhn et al. (2000), using very large datasets of quiet Sun radiances from SUMER and CDS instruments aboard SOHO, showed that the RFDs of VUV lines are much better reproduced by lognormal functions. From this result, the authors suggest that the same heating mechanism is operating in the network and cell centres.

It is, hence, of interest to verify whether the RFD of the optically thick H I Ly-α line also follows a lognormal distribution. Figure 4 shows the quiet Sun normalized RFDs of the four spectral lines here considered. The distributions were created by combining all the data in Table 1 and using a bin size of 0.1 (in units of the average radiance).

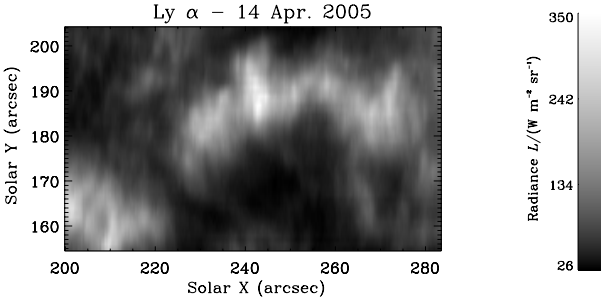

Figure 3: Square-root radiance image of a quiet region near Sun centre. The image was obtained by stepping the slit 0.37"

westward after each exposure, leading to a slightly higher spatial resolution in the direction perpendicular to the slit.

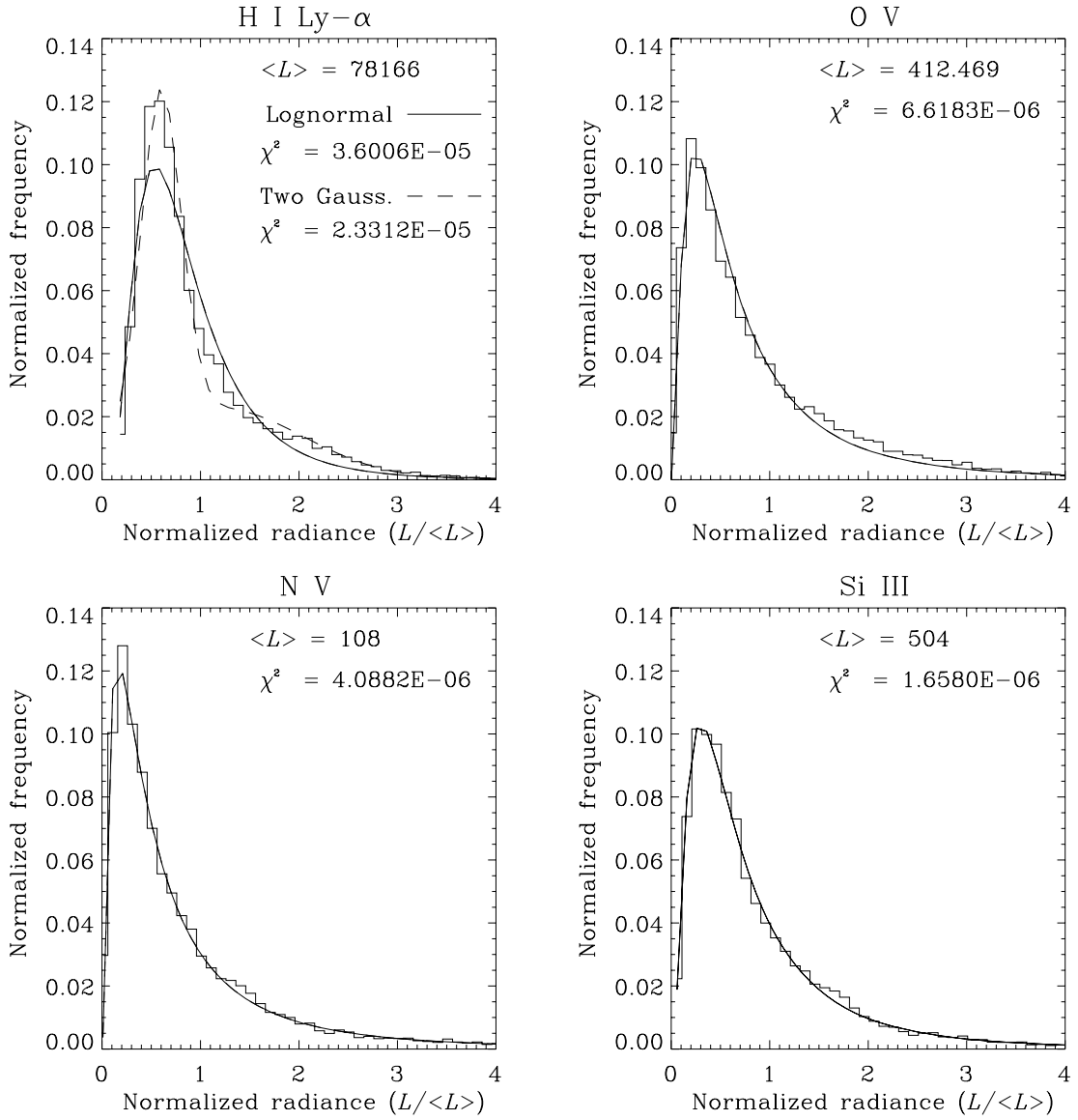

Figure 4. Normalized frequency distributions of the line radiances (in units of the average line radiance) for the four observed lines. The distributions were created combining all the data in Table 1 and using a bin size of 0.1. The average radiances over all the datasets <L> are also given in units of mW m^{-2} sr^{-1}. The Si III, N V and O V radiance frequency distributions (RFDs) are best fitted by a lognormal function while, in the case of H I Ly-α, the lognormal and the double Gaussian fit yield a similar value of χ^2 (see text for details).

The H I Ly-α frequency distribution shows a small bump at normalized radiances around 2 and appears more symmetric than the others. The latter property is in agreement with the behaviour of chromospheric lines reported by Pauluhn et al. (2000). The Si III, N V and O V radiance distributions can be fitted well by a lognormal function (3 free parameters). A double Gaussian fit provides a much worse fit (10 – 20 times larger values of χ^2) despite double the number of free parameters.

Here the χ^2 is defined as the sum over the squared differences between the observed distribution and the fit divided by the number of bins forming the distribution. In the case of the Ly-α radiance distribution, the double Gaussian and the lognormal fit yield a similar value of χ^2. However, the smaller number of free parameters used in fitting a lognormal distribution would make the latter preferable.

5. SIZE OF NETWORK LANES

An estimate of the average size of the network boundaries at a given temperature can be obtained by measuring the full width at half maximum (FWHM) of

the autocorrelation function (ACF) of the radiance map obtained from lines formed at that temperature. This

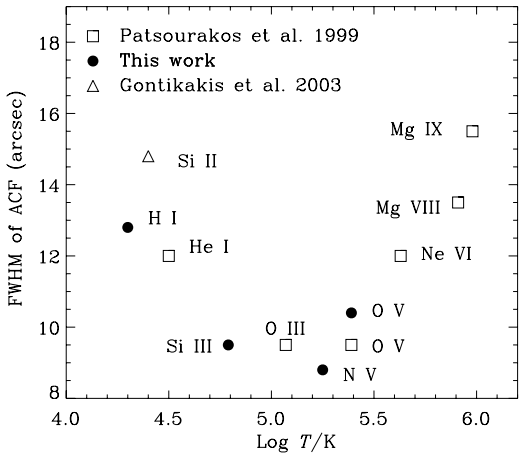

Figure 5. Full width at half maximum (FWHM) of the average autocorrelation functions (ACF) of the radiance distributions along the slit. We notice how the FWHM of the H I Ly-α network is consistent with the values found for lines formed at similar temperatures, either optically thin or thick.

quantity is closely related to the width of the network lanes as seen in the different lines. From such an analysis, Patsourakos et al. (1999) concluded that, for temperatures larger than 2.5×10^5 K the network expands following Gabriel's model. However, these authors also obtained that the network lanes appear larger in He I ($\approx3\times10^4$ K) than in O V (2.5×10^5 K), a result that would be difficult to explain in the framework of magnetic flux tubes expanding with height. They suggested that the larger value found in He I may be due to the sensitivity of this line to coronal back radiation. However, Gontikakis et al. (2003) found the sizes of network lanes to be larger in the optically thin Si II λ153.3 line (2.5×10^4 K) than in the mid TR. These authors explained the smaller mid-TR values as being due to the higher radiance fluctuations shown by lines formed around 10^5 K (see, e.g., Brković et al. 2003).

Figure 5 shows the FWHM of the peak of the ACFs for the lines studied here. It should be noted that the results from Patsourakos et al. (1999) and Gontikakis et al. (2003) are based on radial averages of ACF maps of images (2-D), while here we compute the average ACF of the radiance distributions along the slit. We notice how the FWHM of the network lanes seen in H I Ly-α is consistent with the values found for lines formed at similar temperatures, both optically thin and thick. Thus, the small values obtained for lines formed around temperatures of 10^5 K are very likely due to the higher radiance fluctuations shown by these lines, as suggested by Gontikakis et al. (2003). This could result in an overestimation of the expansion factor calculated by Patsourakos et al. (1999), leading to values more consistent with a smaller flux tube expansion.

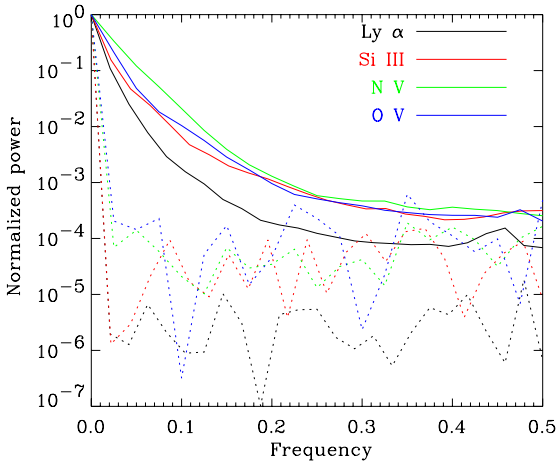

Figure 6. Normalized average power spectra of the radiance distributions along the slit (solid lines). The frequency is the inverse of the spatial scale in pixel units (one SUMER pixel ≈1″). The dotted lines represent the power spectrum of Poisson noise for the average count levels of the various lines.

In general, it should be noted that such an analysis at best shows the expansion of the brightness structures with temperature, i.e., of the locations of high densities of plasma at a given temperature. These sizes, therefore, can tell us something about the distribution of heating but not necessarily follow the expansion of the magnetic field lines.

Figure 6 shows normalized power spectra obtained by averaging the power of the radiance along the slit for each slit position in all datasets of Table 1. Noise power spectra (dotted lines) are also shown. The power spectra show that more power at higher frequencies (small spatial scales) is present in lines with higher formation temperature, confirming the higher dynamics and variability of the mid TR lines. However, it should be noted that the very high signal to noise ratio achievable at H I Ly-α also with short exposure times and/or small apertures, allows smaller spatial and/or temporal variations to be studied better than with any other line in the VUV spectrum. This confirms the huge potential of this line for the investigation of the solar lower TR.

6. CONCLUSIONS

We have obtained spectrally pure raster scan images of quiet Sun regions using the SUMER spectrograph aboard SOHO.

Despite the large opacity characterizing the H I Ly-α line, images obtained in this line look quite similar to those obtained in the optically thin Si III 120.6 nm line. The frequency distribution of H I Ly-α radiance can be approximated by a lognormal function, although the fit

is not so satisfactory as for the optically thin lines formed in the transition region.
The width of the network lanes as seen in H I Ly-α is consistent with that from other lines formed between 20,000 and 30,000 K. Lines formed in the mid-TR apparently indicate smaller widths, but this is likely due to the higher dynamics characterising the TR plasma.
The high S/N ratio achievable with the H I Ly-α line gives the potential to study the very small-scale structure, which is otherwise swamped by noise.

ACKNOWLEDGEMENTS: *The SUMER instrument and its operation are financed by the Deutsches Zentrum für Luft- und Raumfahrt (DLR), the Centre National d'Études Spatiales (CNES), the National Aeronautics and Space Administration (NASA), and the European Space Agency's (ESA) PRODEX programme (Swiss contribution). The instrument is part of ESA's and NASA's Solar and Heliospheric Observatory (SOHO). Part of the data used in this paper was obtained during the SOHO/MEDOC campaign of May-June 2005. L.T. thanks Klaus Wilhelm for suggestions and ideas that helped starting this study.*

REFERENCES

Bonnet R.M. et al. 1980, ApJ, 237, L47
Brković A. Peter H., Solanki S.K., 2003, A&A, 403, 725
Dowdy J.F. Jr., Rabin D., Moore R.L., 1986, Solar Physics, 105, 35
Fontenla J., Reichmann E.J., Tandberg-Hanssen E., 1988, ApJ, 329, 464
Gabriel A., 1976, Phil. Trans. Royal Soc. London, 281, 339
Gontikakis G., Peter H., Dara H.C., 2003, A&A, 408, 473
Korendyke C.M. et al. 2001, Solar Physics, 200, 63
Patsourakos S., Vial J.-C., Gabriel A.H., Bellamine N., 1999, ApJ, 522, 540
Pauluhn A., Solanki S.K., Rüedi I., Landi E., Schühle U., 2000, A&A, 362, 737
Reeves E.M., 1976, Solar Physics, 46, 53
Schrijver C.J. and Title A.M., 2003, ApJ, 597, L165
Tu C.-Y. et al. 2005, Science, 308, 519
Wilhelm et al. 1995, Solar Physics, 162, 189